ORIGINAL ARTICLE

Dual-wavelength erbium-doped fluoride fiber laser

Hongxin Liu[1] · Yongliang Li[1] · Aofei Mao[2] · Chao Yang[1] · Weiwei Hu[1] · Xiaokun Gu[1] · Yipeng Zhang[1]

Abstract
The laser source with 3 μm/2 μm output wavelength has many application prospects in clinical medicine, photoelectric countermeasure, and scientific research measurement. An Er^{3+} doped ZBLAN fiber laser with output wavelength of 2 .8 μm and 1 .6 μm is experimentally studied. By setting the pump power to 5 W, a continuous dual-wavelength output with a central wavelength of 2.803 μm and 1.61 μm is obtained and the corresponding maximum output power is 362.4 mW and 108.6 mW. The slope efficiency is 12.1% and 4.94% respectively. What's more, the slope efficiency is 12.1% and 4.94% respectively, and the fluctuation rates of peak power of the two wavelengths are 9.7% and 2.1% within 4 h which indicate that the laser has relatively good stability.

Keywords Fiber laser · Er-doped fluoride · Cascaded mode · 2.8 μm/1.6 μm

Introduction

Laser source with output of 3 μm/2 μm has a wide range of applications in industrial processing, measurement, scientific research, military and civil fields, and especially biomedical [1–7]. About 70% of human tissues are composed of water. The infrared absorption spectrum of water shows that it has a strong absorption peak at 3- and 2-μm bands, so laser with wavelength of 3 μm/2 μm can be used to remove the necrotic structure of human body and to perform minimally invasive surgery [8–12].

For practical applications, there are mainly three ways to obtain laser at Nonlinear performance: (1) semiconductor lasers with gain media of narrow-band compounds of aluminum, gallium, arsenic, and antimony [13–15]; (2) using nonlinear performance of some crystal materials to transfer the long-infrared or short-infrared bands can to near-infrared and medium-infrared bands [16, 17]; (3) near-mid-infrared fiber laser with lanthanide-doped fluorides, sulfides, and oxide materials as gain medium [18–26].

In order to achieve dual-wavelength output of 3 μm and 2 μm, two methods are often used in the laboratory. First, the laser of these two wavelengths is produced by using two independent resonator structure, and then couple into a beam by using an optical fiber integrator. This method requires two laser oscillator and two pumping sources. The structure is complicated and the operation is inconvenient which greatly limit its application in medicine [27]. Second, cascaded oscillator fiber lasers can not only obtain two-band laser output from the only one resonator, reducing the space volume, but also achieve large-scale and high-efficiency laser power output [28–31]. In this paper, the cascaded oscillation mode is used to explore the dual-band erbium-doped fluoride fiber laser which can be used for further experiment and application.

Theory analysis

Energy level analysis

Cascade oscillation can deliminate the self-termination effect of the light source, and the doping concentration of Er^{3+} ion in the optical fiber is reduced to less than at.1%. The energy level diagram of the dual-wavelength cascaded Er^{3+}: ZBLAN fiber laser is shown in Fig. 1 [32]. Er^{3+} ions are stimulated from the laser high-level $^4I_{13/2}$ to the ground state $^4I_{15/2}$, irradiating a 1.6-μm beam, resulting in the rapid depletion of the ions

✉ Yongliang Li
liyongliang1973@163.com

[1] The School of Opto-electronics Engineering, Changchun University of Science and Technology, Changchun 130022, Jilin, China

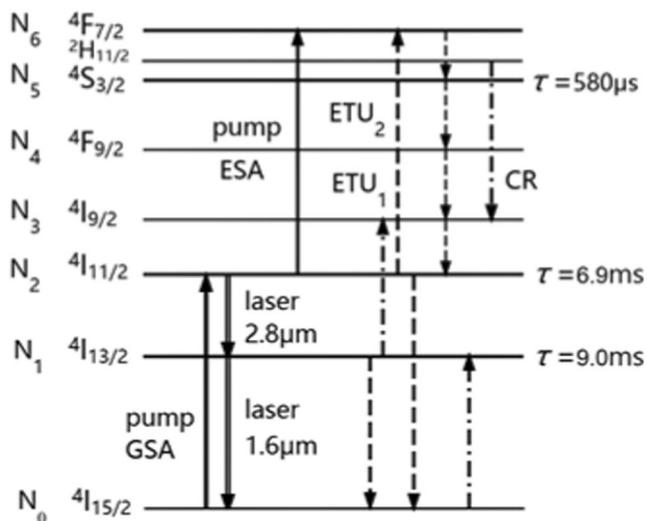[2] Department of Electrical and Computer Engineering, University of Nebraska-Lincoln, Lincoln, NE 68503, USA

Fig. 1 Energy band diagram of Er^{3+}: ZBLAN fiber laser

retained at the $4I_{13/2}$ level which ensures the ion number inversion between the $4I_{11/2}$ level and the $4I_{13/2}$ level. Therefore, the critical pump interval is reduced at 2.8-μm wavelength, promoting the output of 2.8-μm beam. What's more, as for $^4I_{11/2}$ level, ETU_2 consumes the particles on it and increases the difficulty of population inversion for 2.8-μm laser. The excitation threshold at a wavelength of 1.6-μm. In addition, ETU_1 will also reduce the $4I_{13/2}$ level ion number and further increase the threshold for 1.6-μm beam. In a sentence, the ETU_2 process has a negative effect on the ion inversion of both 1.6-μm and 2.8-μm. On the contrary, the ETU_1 process is beneficial to the excitation of 2.8-μm, but not to the excitation of 1.6-μm. For Er^{3+}: ZBLAN fiber, the ETU_2 process has a long time to play its role, significantly exceeding the ETU1 process. If the negative effect caused by the ETU_2 process is to be greatly reduced, the mixing ratio of Er^{3+} ions in cascade mode should be lowered.

Rate equation

There is more than one mode of quasi-monochromatic during laser oscillation. Each mode has a certain frequency and cavity loss. In order to simplify the problem, we only discuss the number l's oscillation mode in the laser system.

The derivative equation of the atom's relative time of each level is:

$$\frac{dn_3}{dt} = n_1 W_{13} - n_3(S_{32} + A_{31} + S_{31})$$
$$\frac{dn_2}{dt} = n_1 W_{12} - n_2 W_{21} - n_2(A_{21} + S_{21}) + n_3 S_{32} \quad (1.1)$$
$$n_1 + n_2 + n_3 = n$$

The photon number in the oscillation cavity is represented by N_l, and the photon lifespan is τ_{Ri}. The equation

representing the change of the number of photons can be written as follows:

$$\frac{dN_l}{dt} = n_2 W_{21} - n_1 W_{12} - \frac{N_l}{\tau_{Rl}} \quad (1.2)$$

Substituting W_{21} and W_{12} with the stimulated emission cross sections and the stimulated absorption, the rate equations can be rewritten as follows:

$$\frac{dn_3}{dt} = n_1 W_{13} - n_3(S_{32} + A_{31})$$
$$\frac{dn_2}{dt} = -\left(n_2 - \frac{f_2}{f_1}n_1\right)\sigma_{21}(\nu,\nu_0)\upsilon N_l - n_2(A_{21} + S_{21}) + n_3 S_{32}$$
$$n_1 + n_2 + n_3 = n$$
$$\frac{dN_l}{dt} = \left(n_2 - \frac{f_2}{f_1}n_1\right)\sigma_{21}(\nu,\nu_0)\upsilon N_l - \frac{N_l}{\tau_{Rl}}$$
$$(1.3)$$

where $\eta_1 = S_{32}/(S_{32} + A_{31})$, which is the quantum efficiency of radiation-free transition from E_3 to E_2, $\eta_2 = A_{21}/(A_{21} + S_{21})$, which is the fluorescence efficiency of E_2 to E_1 level, the total quantum efficiency is η_F, which equals to $\eta_1\eta_2$. Therefore, the rate equation can also be described as:

$$\frac{dn_3}{dt} = n_1 W_{13} - \frac{n_3 S_{32}}{\eta_1}$$
$$\frac{dn_2}{dt} = -\left(n_2 - \frac{f_2}{f_1}n_1\right)\sigma_{21}(\nu,\nu_0)\upsilon N_l - \frac{n_2 A_{21}}{\eta_2} + n_3 S_{32} \quad (1.4)$$
$$n_1 + n_2 + n_3 = n$$
$$\frac{dN_l}{dt} = \left(n_2 - \frac{f_2}{f_1}n_1\right)\sigma_{21}(\nu,\nu_0)\upsilon N_l - \frac{N_l}{\tau_{Rl}}$$

In this system, the formation modes of the beams are different. First, the E_2 level is regarded as a relatively stable level, the E_3 level is an upper level, and the fluorescence is formed from the E_3 to E_2 level; second, the E_1 level is regarded as a beam low level, the E_2 level is an upper level, and the fluorescence is formed from the E_2 to E_1. The difference in luminescence mechanism leads to the difference in the excitation form of the gain material.

Experiment

Experiment setup

The pump source used in the experiment is 976 nm fiber coupled output semiconductor laser. The reflectivity of dichroic mirrors used in the study is higher than 99% in 976 nm, and the transmittance at 3 μm and 2 μm is higher than 98%. The transmittance of the planar cavity mirror near the pump light is higher than 99%, and the reflectivity is 5% at 3 μm, while 42% at 2 μm. The totally reflecting mirror applied

Fig. 2 The spectra of dichroic mirrors and planar mirrors

Reflection spectrum of dichroic mirror

Reflection spectrum of planar mirrors
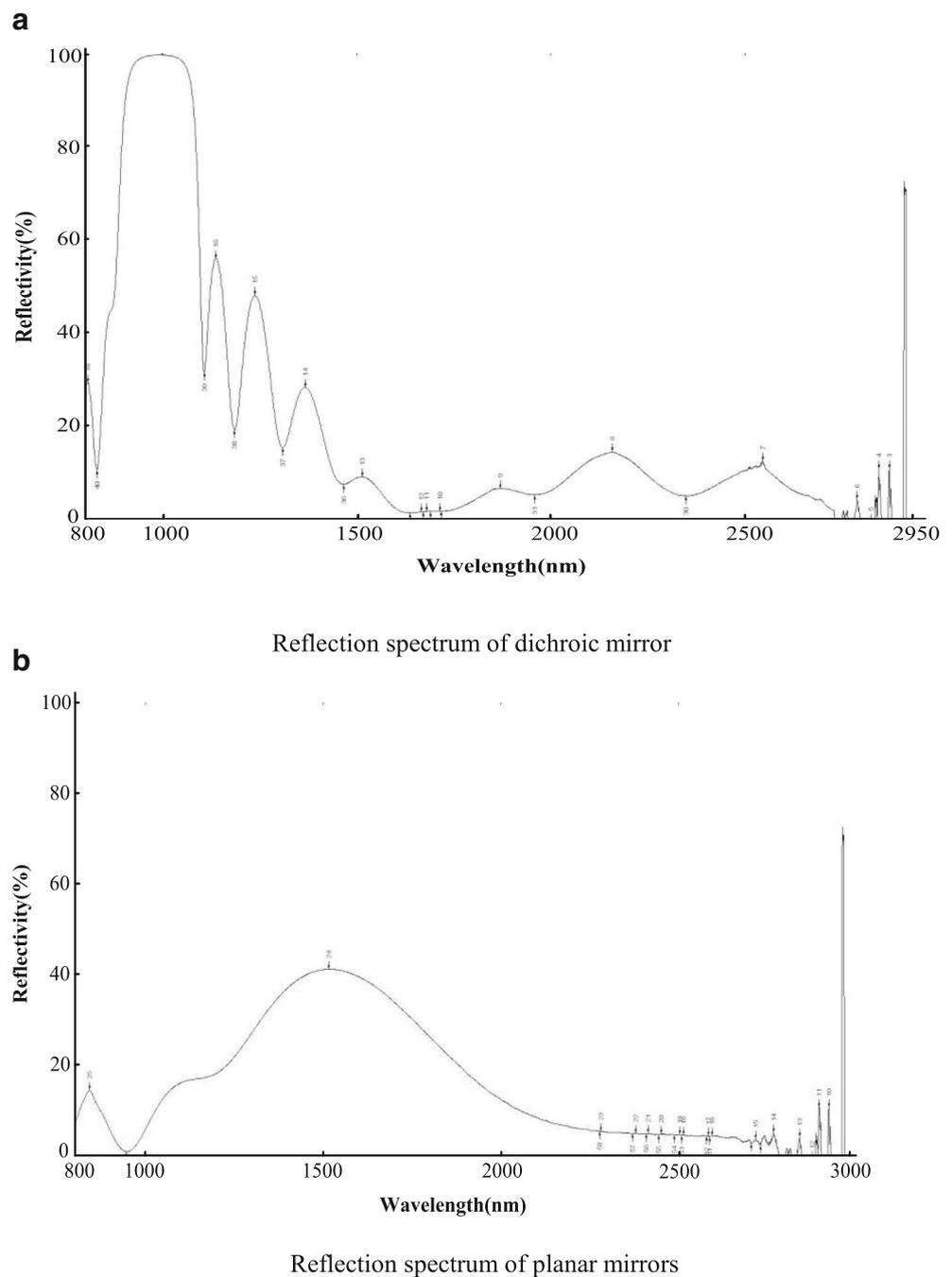
in the other end is a gold-plated planar mirror. The spectra of dichroic mirrors and planar mirrors are shown in Fig. 2.

For resonator structure of Er^{3+}: ZBLAN cascaded fiber laser, we still use the traditional F-P resonator, as shown in Fig. 3. Pumped light, a high-power LD laser with a center wavelength of 976 nm, passes through a core fiber with a diameter of 200 μm and a length of 1 m. Then, a set of colli-mated focusing lenses with focal length of 100 mm is used to couple the pumped light into fiber. This lens group has a transmittance of more than 98% to the pump light. A dichroic mirror is put 45° incline with laser beam. In this case, a very small space between the input cross-section of the optical fiber and the front cavity plane mirror is required to ensure that the coupling ratio of the pump light is increased as far as possible without damaging the coating surface of the plane mirror and the cross-section of the optical fiber. The gold-plated totally

Fig. 3 Experiment setup of cascaded Er^{3+}: ZBLAN fiber laser
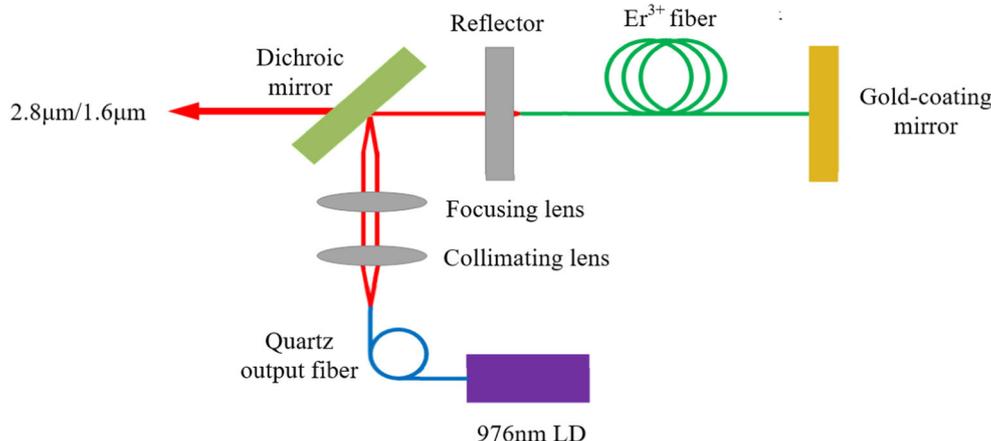
reflecting mirror closed to the other end of the optical fiber is used as a component of the resonator to provide optical feedback. As the gain of laser oscillation exceeds loss, signal light will be transmitted from the plane mirror and dichroic mirror.

During the whole experiment, the dichroic mirror and the plane mirror are both input and output ends. Both ends of the gain fiber are fixed on a circular rotating bracket to adjust the angle between the fiber end face and the two resonant cavity mirrors. The end face is cut vertically. The whole device is run at room temperature without any active water-cooling device (Fig. 4).

Results and analysis

Figure 5 shows the variation of output power of the two wavelengths with the pump power. It can be seen that the 3-μm laser is generated when pump power is 0.8 W, and the output power of the 3-μm laser rises linearly with the increase of the pump power. When pump power is 2.8 W, the 2-μm laser formed, and at this moment, the emission power of 3-μm laser

is 96.3 mW, the corresponding slope ratio is 4.82%. Continuously, the output power of the 3- and 2-μm band laser increases linearly with the increase of pump power up. To be noticed, the output power of the 3-μm laser changes when the 2-μm laser is generated. This is because the generation of 2-μm band cascaded signal light reduces the number of Er^{3+} ions in the 3-μm band level very well, and then increases the output power. When the pump power increases to a maximum of 5 W, the output power of the 3-μm laser and 2-μm laser is 362.4 mW and 108.6 mW respectively. The Slope ratio is 12.1% and 4.94% which is improved significantly compared with the slope ratio before .

The signal of the 2.8-μm laser can be observed from the output spectra when pumping power reaches 0.8 W, but the spectral intensity is weak. After continuously increasing the pump power, the peak value of the laser will gradually increase. When pumping power exceeds 2.8 W, the cascaded signal of 1.6 μm will be generated, while the peak value of the cascade wavelength is not obvious due to the influence of noise. When the pump power is increased to the maximum of 5 W, the spectrum intensity of the two lasers reaches the
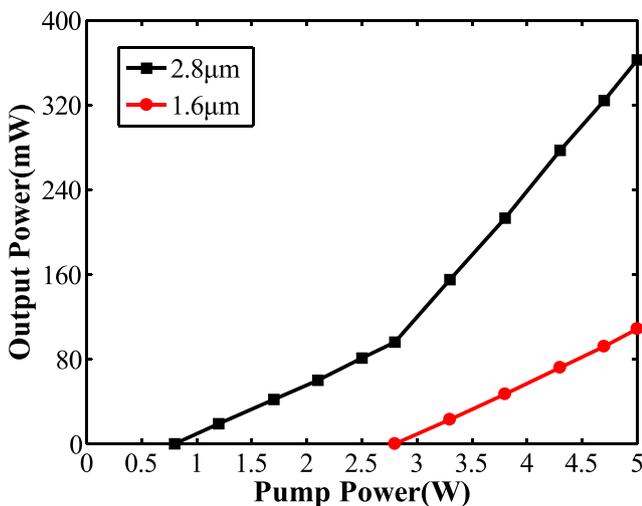

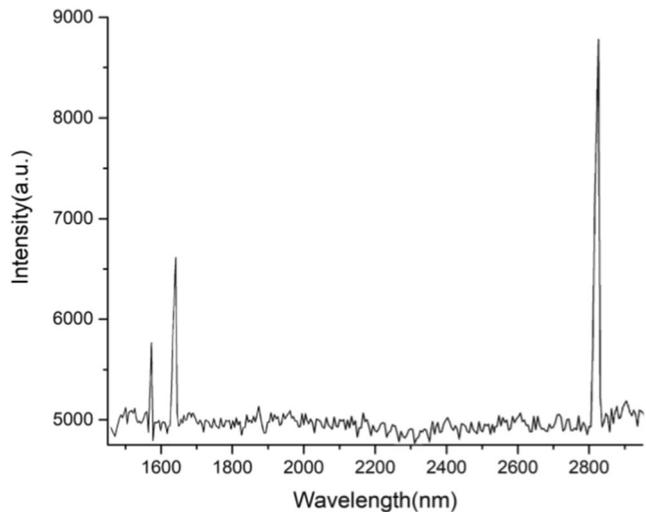**Fig. 4** Curves of laser output power versus pump power

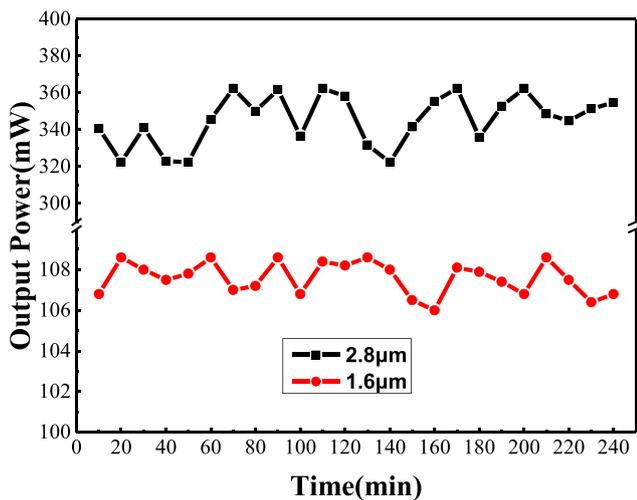**Fig. 5** Output spectrum when pumping power at 5 W

Fig. 6 Stability of output power at maximum pumping power

laser output were obtained simultaneously. The corresponding slope efficiencies were 4.94% and 12.1% respectively. Experiments show that the cascade mode is helpful to reduce the laser threshold of 2 .8 μm, thus greatly increasing the output power of 3-μm band laser and improving the stability of the output laser.

Compliance with ethical standards

Conflict of interest The authors declare that they have no conflict of interest.

Ethical approval Ethics approval was not needed.

maximum. Figure 6 shows the stable output spectrum when pumping power equals to 5 W (APE Mid infrared spectrometer, wavelength range 1500–6300 nm, resolution 3 nm).

As shown in Fig. 5, the spectral intensity of 2.8 μm is much higher than that of 1.6 μm, which is the result of rapid reduction of the number of ions on the $4I_{13/2}$ level by the emitted cascade signal light. Meanwhile, two distinct signal beams appeared near 1.6 μm, one at about 1550 nm and the other at about 1610 nm which is dominated over 1550 nm. It is supposed that if the pump power of the cascaded Er3 +: ZBLAN fiber laser system is increased again, the oscillation mode near 1550 nm may be inhibited. When the pump power equals to 5 W, the central wavelength of 2.8 μm laser is 2803 nm and the bandwidth is 4.37 nm. The central wavelength of 1.6-μm laser is 1610 nm and the bandwidth is 5.42 nm. In addition, because of the energy up-conversion and stimulated absorption process, bright green light will be formed after the pumping light is absorbed by the Er^{3+} doped ZBLAN fiber. This phenomenon can help us understand the transmission of pumped light in the fiber and briefly judge the pumping efficiency of the pumping light.

Finally, the output stability of these two wavelengths at the maximum pump power is tested. As shown in Fig. 6, the time interval is 10 min and the total time is 4 h. From the floating curve, we can see that the fluctuation rate of the output power of 2.8 μm is 9.7%, and that of the output power of 1.6 μm is 2.1%.

Conclusion

A cascaded Er^{3+}: ZBLAN fiber laser system was constructed in this experiment. The 3-μm and 2-μm dual-band laser output experiments were successfully completed. The stable dual-wavelength output of 1610 nm and 2803 nm was obtained. When the pumping power is 5 W, 108.6- and 362.4-mW

References

1. Chen W, Han Z, Shi H et al (2017) Widely wavelength tunable gain-switched Er³⁺-doped ZBLAN fiber laser around 2.8μm. Opt Express 25(8):8816
2. Tang P, Wu M, Wang Q et al (2016) 2.8μm pulsed Er³⁺:ZBLAN fiber laser modulated by topological insulator. IEEE Photon Technol Lett 28(14):1573–1576
3. Arora H, Falto-Aizpurua L, Chacon A et al (2015) Lasers for nevi: a review. Lasers Med Sci 30(7):1991–2001
4. Al-Karadaghi TS, Franzen R, Jawad HA et al (2015) Investigations of radicular dentin permeability and ultrastructural changes after irradiation with Er,Cr:YSGG laser and dual wavelength (2780 and 940 nm) laser. Lasers Med Sci 30(8):2115–2121
5. Khamis MA, Ennser K (2017) Enhancement on the generation of amplified spontaneous emission in thulium-doped silica fiber at 2μm. Opt Commun 403:127–132
6. Jobin F, Maes F, Bernier M et al (2017) Diode-pumped mid-infrared fiber laser with 50% slope efficiency. Optica 4(2):235
7. Sergei A, Darren DH, Alexander F et al (2016) High-power mid-infrared femtosecond fiber laser in the water vapor transmission window. Optica 3:1373
8. Bayly JG, Kartha VB, Stevens WH (1963) The absorption spectra of liquid phase H₂O, HDO and D₂O from 0.7μm to 10μm. Infrared Physics 3(4):211~222
9. Wei C, Zhu X, Norwood RA et al (2012) Passively Q-switched 2.8-mum nanosecond fiber laser. IEEE Photon Technol Lett 24(19): 1741–1744
10. Hu T, Hudson DD, Jackson SD (2012) Actively Q-switched 2.9μm Ho³⁺/Pr³⁺-doped fluoride fiber laser. Opt Lett 37(11):2145~2147
11. Tokita S, Murakami M, Shimizu S, et al. 12W Q-switched Er: ZBLAN fiber laser at 2.8μm. Opt Lett, 2011, 36(15): 2812~2814
12. Maes F, Fortin V, Bernier M et al (2017) 5.6W monolithic fiber laser at 3.55μm. Opt Lett 42(11):2054
13. Ongstad AP, Kaspi R, Dente GC et al (2007) Midinfrared, optically pumped, unstable resonator lasers. Appl Phys Lett 90(19):191107
14. Ongstad AP, Dente GC, Tilton ML et al (2010) High brightness from unstable resonator mid-IR semiconductor lasers. J Appl Phys 107(12):123113

15. Yang C, Paxton AH, Newell TC et al (2017) On-chip unstable resonator cavity GaSb-based quantum well lasers. J Appl Phys 121(14):3146

16. Chang J, Mao Q, Feng S et al (2010) Widely tunable mid-IR difference-frequency generation based on fiber lasers. Opt Lett 35(20):3486–3488

17. Sobon G, Krzempek K, Abramski KM (2013) DFG-based mid-IR generation using a compact dual-wavelength all-fiber amplifier for laser spectroscopy applications. Opt Express 21(17):20023–20031

18. Arbazzadah E, Chard S, Amrania H et al (2011) Comparison of a diode pumped Er:YSGG and Er:YAG laser in the bounce geometry at the 3μm transition. Opt Express 19(27):25860–25865

19. Martyshkin DV, Moskalev IS, Mirov MS et al (2011) Progress in mid-IR Cr^{2+} and Fe^{2+} doped II-VI materials and lasers. Opt Mater Express 1(5):898~910

20. Fried NM, Yang Y, Chaney CA et al (2004) Transmission of Q-switched erbium:YSGG (λ=2.79μm) and erbium:YAG (λ=2.94μm) laser radiation through germanium oxide and sapphire optical fibres at high pulse energies. Lasers Med Sci 19(3):155–160

21. Luo Z, Liu C, Huang Y et al (2014) Topological-insulator passively Q-switched double-clad fiber laser at 2μm wavelength. IEEE J Quantum Electron 20(5):1–8

22. Liu J, Xu J, Wang P (2012) Graphene-based passively Q-switched 2μm thulium-doped fiber laser. Opt Commun 285(24):5319–5322

23. Zhu G, Zhu X, Balakrishnan K et al (2013) Fe^{2+}:ZnSe and graphene Q-switched singly Ho^{3+}-doped ZBLAN fiber lasers at 3μm. Opt Mater Express 3(9):1365–1377

24. Hendersonsapir O, Munch J, Ottaway DJ (2014) Mid-infrared fiber lasers at and beyond 3.5μm using dual-wavelength pumping. Opt Lett 39(3):493~495

25. Zhang J, Wang N, Guo Y et al (2018) Tm^{3+}-doped lead silicate glass sensitized by Er^{3+} for efficient ~2μm mid-infrared laser material. SPECTROCHIM ACTA A 199:65–70

26. Pratisto H, Frenz M, Ith M et al (1996) Combination of fiber-guided pulsed erbium and holmium laser radiation for tissue ablation under water. Appl Opt 35(19):3328~3337

27. Sumiyoshi T, Sekita H, Arai T et al (1999) High-power continuous-wave 3 and 2μm cascade Ho^{3+}: ZBLAN fiber laser and its medical applications. IEEE J Quantum Electron 5(4):936~943

28. Li J, Hu T, Jackson SD (2012) Q-switched induced gain switching of a two-transition cascade laser. Opt Express 20(12):13123

29. Tsai TY, Fang YC, Tsao HX et al (2012) Passively cascade-pulsed erbium ZBLAN all-fiber laser. Opt Express 20(12):12787–12792

30. Jackson SD, Pollnau M, Li J (2011) Diode pumped erbium cascade fiber lasers. IEEE J Quantum Electron 47(4):471–478

31. Razeghi M, Bandyopadhyay N, Bai Y et al (2013) Recent advances in mid infrared (3-5μm) quantum cascade lasers. Opt Mater Express 3(11):1872–1884

32. Li J, Hudson DD, Jackson SD (2011) High-power diode-pumped fiber laser operating at 3μm. Opt Lett 36(18):3642–3644